Geophysical Research Letters

RESEARCH LETTER
10.1029/2020GL087679

Key Points:
- The Indonesian throughflow inflow and outflow profiles resolved by reanalysis products display different correlations to climate indices
- The thermocline inflow responds to the El Niño-Southern Oscillation (ENSO) signal with almost no lag, while the outflow lags ENSO by 5–7 months
- The sub-thermocline inflow and outflow respond to the Interdecadal Pacific Oscillation (IPO) with 7–13 months lag and show long-term trends

Supporting Information:
- Supporting Information S1

Correspondence to:
A. L. Gordon,
agordon@ldeo.columbia.edu

Citation:
Li, M., Gordon, A. L., Gruenburg, L. K., Wei, J., & Yang, S. (2020). Interannual to decadal response of the indonesian throughflow vertical profile to Indo-Pacific forcing. *Geophysical Research Letters*, *47*, e2020GL087679. https://doi.org/10.1029/2020GL087679

Received 25 FEB 2020
Accepted 28 APR 2020
Accepted article online 29 APR 2020

Interannual to Decadal Response of the Indonesian Throughflow Vertical Profile to Indo-Pacific Forcing

Mingting Li[1,2], Arnold L. Gordon[3], Laura K. Gruenburg[3], Jun Wei[1,2], and Song Yang[1,2]

[1]School of Atmospheric Sciences and Guangdong Province Key Laboratory for Climate Change and Natural Disaster Studies, Sun Yat-sen University, Guangzhou, China, [2]Southern Marine Science and Engineering Guangdong Laboratory (Zhuhai), Zhuhai, China, [3]Lamont-Doherty Earth Observatory, Columbia University, New York City, NY, USA

Abstract The Indonesian Throughflow (ITF) inflow through the Sulawesi, Maluku, and Halmahera Seas and the ITF outflow into the eastern tropical Indian Ocean, based on reanalysis and model data, are used to investigate the interannual to decadal response of the ITF vertical profile to Indo-Pacific forcing. The thermocline (upper 300 m) inflow, driven by the North Pacific Ocean, negatively responds to El Niño-Southern Oscillation (ENSO) with almost no lag; while the thermocline outflow lags by 5–7 months. The sub-thermocline (300–760 m) inflow, which is influenced by both the North and South Pacific, positively responds to ENSO and Interdecadal Pacific Oscillation (IPO) indices with 13 months lag and displays a long-term trend tracking the IPO index. Influenced by eastern Indian Ocean variations, the sub-thermocline outflow positively correlates with the ENSO and IPO indices with about 7–9 months lag, a shorter lag time than the inflow.

Plain Language Summary The vertical structure of the Indonesian Throughflow (ITF) plays an important role in modulating the Indo-Pacific Ocean freshwater and heat content. The response time of the thermocline and sub-thermocline ITF to Indo-Pacific climate indices differs as the two layers are related to variations in different geographic regions. Thermocline layer inflow responds to the interannual ENSO signal with almost no lag, with 5–7 months lag for outflow. The sub-thermocline layer is related to decadal time scales. The increased ITF during periods of La Niña contributed to the Indian Ocean heat content increasing in the past decade. Changes in the ITF vertical velocity profile are important for Indo-Pacific Ocean heat exchange, which is likely to be altered due to global climate change. The results have important implications for investigating the influences of ITF vertical profile on the interannual to decadal Indian Ocean circulation changes.

1. Introduction

The Indonesian throughflow (ITF), driven by the pressure gradient between the Pacific and Indian Oceans (Wyrtki, 1987; Clarke & Liu, 1994;), transfers water from the tropical Pacific Ocean to the Indian Ocean, affecting the heat and freshwater inventories of both oceans and modifying ocean-atmosphere exchanges in the Indo-Pacific warm pool (Gordon, 1986, 2001; Gordon et al., 2003; Gruenburg & Gordon, 2018; Hu et al., 2015; Lee et al., 2015; Sprintall et al., 2014). The pressure difference between the Pacific and Indian Oceans, maintained by trade winds over the Pacific Ocean and monsoon winds over the Indian Ocean, governs the lower frequencies of the ITF (Potemra & Schneider, 2007; Sprintall et al., 2009; Wyrtki, 1965). The El Niño-Southern Oscillation (ENSO) phenomenon and Indian Ocean Dipole (IOD) are the primary climate modes effecting the ITF at interannual time scales (Gordon et al., 1999; 2012; Yuan et al., 2011, 2013; Liu et al., 2015; Gordon et al., 2019; Pujiana et al., 2019). Observations and numerical experiments indicated that the ITF transport across the IX1 section on the Indian Ocean side of the Indonesian Seas is larger during La Niña and positive IOD events (Gordon et al., 2019; Masumoto, 2002; Murtugudde et al., 1998; Potemra & Schneider, 2007; Sprintall & Révelard, 2014). The correlation between the filtered IX1 section transports (ITF outflow) and Dipole Mode Index (DMI, the IOD index) is −0.35, with the DMI leading ITF about 1–3 months (Yuan et al., 2013). ITF total outflow transport across the IX1 section lags Niño 3.4 by about 7 months (Liu et al., 2015; Yuan et al., 2013). ENSO and IOD affect the ITF through propagation of equatorial Kelvin and Rossby waves adjusting the Pacific/Indian pressure gradient (Pujiana et al., 2013, 2019; Sprintall et al., 2000; Yuan et al., 2011, 2013). The IOD is well correlated with ENSO, but about a third of IOD events occur independently of ENSO (Cai et al., 2012; Stuecker et al., 2017). As an ocean pathway relating tropical Pacific and Indian Oceans, the ITF also plays a role in interactions between ENSO and IOD (Santoso et al., 2011; Yuan et al., 2013).

The decadal variability of ITF is related to the Interdecadal Pacific Oscillation (IPO), the Pacific Decadal Oscillation (PDO), and trends in North Pacific trade winds (Feng et al., 2011, 2018; Li et al., 2018; Tillinger & Gordon, 2010). Global climate change in the past two decades has caused an increase in the trade winds over the Pacific Ocean, strengthening the ITF and increasing the upper layer heat content of the Indian Ocean (England et al., 2014; Lee et al., 2015; Nieves et al., 2015). Climatic changes causing rainfall intensification affect surface salinity within the Indonesian Seas and have played an important role in the interannual to decadal variability of ITF in past decades (Hu & Sprintall, 2017). The salinity effect propagates from the Indonesian Seas to eastern tropical Indian Ocean and then feeds back onto ITF transport variability, which contributes to about 36% of the interannual variability of the ITF (Hu & Sprintall, 2016).

Pacific water flows into the Indonesian Seas through Sulawesi Sea-Makassar Strait, the western pathway, and through Maluku and Halmahera Sea, the eastern pathway (Gordon & Fine, 1996; Yuan et al., 2018). The ITF contributes a relatively cool and low salinity water mass to the Indian Ocean thermocline through the Timor Passage and the Ombai and Lombok Straits (Atmadipoera et al., 2009; Gordon et al., 2003; Gordon et al., 2010; Sprintall et al., 2009; Sprintall et al., 2014). The shape of the ITF vertical profile has implications for Indian Ocean stratification and heat fluxes in the eastern tropical Indian Ocean (Song & Gordon, 2004). However, the interannual to decadal variability of the ITF vertical profile is not as well defined. From 13 years of mooring data (2004–2011, 2013–2017) within the Makassar Strait (major pathway of ITF, with approximately 12 Sv southward flow and comprising about 80% of the total ITF, Gordon et al., 2019), we acquire further insight into the fluctuations of the vertical profile of the ITF including evidence of anomalous events. The observed ratio of upper 300 m to 300–760 m Makassar Strait transport displays anomalous behavior, attaining a near 1:1 ratio after the 2015/16 El Niño event in comparison to the long term (2004–2017) ratio of 3:1 (Gordon et al., 2019). This implies that different mechanisms are driving the currents in the thermocline (0–300 m) and sub-thermocline (300–760 m) layers. In this study we examine the Pacific Ocean inflow and Indian Ocean outflow of ITF and investigate the relationship of the inflow and outflow transports of ITF in the thermocline and sub-thermocline layers to Indo-Pacific climate forcing.

2. Data and Methods

Mooring data in the Makassar Strait, located within the Labani Channel near 3°S (Figure 1a) from January 2004 to August 2011 and August 2013 to August 2017 (Gordon et al., 2019), was used to calculate the transport time series for the Makassar Strait Throughflow (MST; Gordon et al., 2003, 2008; Susanto et al., 2012). To study interannual and decadal changes and the response of the ITF profile to Indo-Pacific climate forcing over longer periods than covered by the MST timeseries, we define inflow sections at the Sulawesi Sea (125°E, 1°N–6°N), Maluku Sea (125°E–127.5°E, 0.5°N), and Halmahera Sea (128°E–131°E, 0.5°S), and an eastern tropical Indian Ocean outflow section (114°E, 8°S–22°S) all marked in Figure 1a (black and green lines). The inflow and outflow transports are calculated from monthly NCEP Global Ocean Data Assimilation System (GODAS) and Simple Ocean Data Assimilation (SODA) 3.12.2 reanalysis data, as well as Ocean General Circulation Model for the Earth Simulator (OFES) output from 1980 to 2017 (supporting information Figure S1). All these data sets have been shown to provide a good simulation of the western Pacific Ocean circulation (Figure S2) and have been used in many studies (Du & Qu, 2010; Duan et al., 2019; Masumoto et al., 2004; Ren et al., 2018; Tillinger & Gordon, 2010; Wang & Wu, 2013). The three timeseries are averaged for each section and smoothed with a 13-month running mean to remove the seasonal variations. These ensemble mean inflow and outflow timeseries based on GODAS, SODA3, and OFES data sets are used for the following analysis (red lines in Figures 1b–1e).

To validate the ensemble ITF inflow and outflow transports timeseries, three timeseries from previous studies were used. The first uses eXpendable Bathy Thermography (XBT) measurements along section IX1 (red scatter in Figure 1a, Liu et al., 2015; Feng et al., 2018) to calculate the geostrophic transport of ITF outflow. The second is an ITF geostrophic transport out of the Indonesian Australian Basin during 1962–2010 created

10.1029/2020GL087679

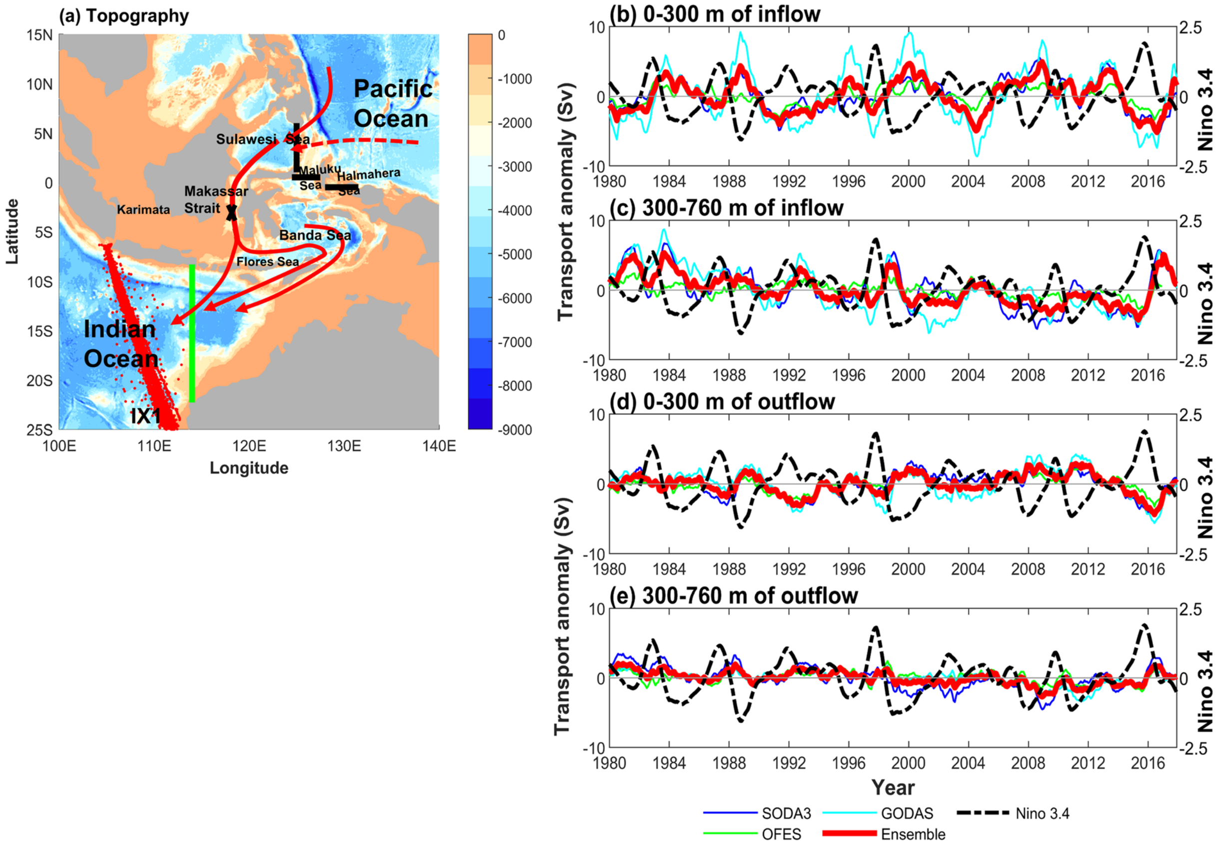

FIGURE 1. (a) Topography of Indonesian Seas, with the ITF pathways presented by the red arrows, and mooring site marked by black X in the Makassar Strait. The dash red arrow shows the pathway of Pacific water into Sulawesi Sea in the sub-thermocline layer. The solid black and green lines indicate the positions of the inflow and outflow sections, respectively. Section IX1 is marked with red scatter. (b)13-month running mean inflow transport anomaly at thermocline layer calculated from GODAS (black line), SODA3 (blue line), OFES (green line) data sets, and the ensemble mean of these three datasets (red line). (c) Same as (b) but for sub-thermocline layer. (d and e) Thermocline and sub-thermocline transport anomalies across the outflow section. Positive values denote more southward or westward transport.

by Hu and Sprintall (2016, 2017). The third is a 68 year (1948–2016) upper 300 m MST timeseries constructed by Li et al. (2018) using neural network fitting based on mooring data and North Pacific zonal winds. The Indo-Pacific climate modes, Niño 3.4, IOD, PDO, and IPO indices are all products of NOAA Earth System Research Laboratory (ESRL).

3. Results and Discussion

With 38-year timeseries of inflow and outflow data, we can investigate the interannual to decadal response of the thermocline (0–300 m) and sub-thermocline (300–760 m) transport to regional climate forcing. The thermocline layer timeseries shows larger interannual variability than does the sub-thermocline layer (Figures 1b–1e), while the sub-thermocline layer shows larger decadal variability than the thermocline layer. In the frequency domain the thermocline inflow timeseries shows peak energy in periods of 2–7 years, while sub-thermocline inflow and outflow also peak in periods greater than 10 years, on similar time scales to IPO and PDO indices (Figure S3). Total inflow of ITF includes the eastern (through Maluku Sea and Halmahera Sea) and western pathways (through Sulawesi Sea-Makassar Strait). Based on the INSTANT observations from 2004 to 2006, the average MST provides about 80% of the total ITF into the Indian Ocean, though the yearly percentage varied from approximately 74% to 81% (Table 1 of Gordon et al., 2010). The remaining ~20% of the ITF is drawn mostly from the eastern pathways of the Indonesian Seas (Gordon et al., 2010). Results from the reanalysis are consistent with these observations, the eastern pathway transport is about −3 Sv, while the western pathway is −13 Sv (Figure S4). The western pathway, beginning at the Sulawesi Sea section, contributes almost all variability to the total inflow. The correlation coefficients between the

Sulawesi Sea section and the total inflow from SODA3 within the 99% confidence interval are 0.96 in the thermocline layer and 0.93 in the sub-thermocline layer. The comparison of the 13-year observed MST timeseries (Figures 2a and 2b) to the ensemble inflow finds a significant correlation coefficient of 0.74 (thermocline) and 0.83 (sub-thermocline). This and all further correlation coefficients discussed are significant to the 95% confidence interval. The ensemble outflow transport timeseries also has high correlation coefficient ($r = 0.83$ of the thermocline and $r = 0.75$ of the sub-thermocline) with observed MST timeseries, which indicates that the multidecadal inflow and outflow timeseries can serve as proxies for ITF.

For further validation, we compare the ensemble inflow and outflow in the thermocline layer (Figures 2c–2e) to the upper 400 m XBT-IX1 transport between Western Australia and Java (Feng et al., 2018; Liu et al., 2015; Wijffels et al., 2008). The thermocline layer outflow is well correlated ($r = 0.7$, 1–2 months lead) with the XBT-IX1 timeseries, and the inflow leads about 5–6 months with $r = 0.6$. These two timeseries diverge notably only during 1984–1987. The ITF time series from Hu and Sprintall (2016) also compares well to the inflow ($r = 0.67$, about 10 months lag) and outflow ($r = 0.65$, about 2 months lag). Constructed multidecadal timeseries of 0–300 m MST from Li et al. (2018) is also compared to the total inflow and outflow transport. Ensemble inflow leads the constructed ITF time series about 2–3 months with $r = 0.42$ and the outflow lags about 2–3 months with $r = 0.55$.

The thermocline transport of ITF inflow has a negative correlation ($r = -0.65$) with zero lag to the Niño 3.4 (Figure 3a), which indicates decreased inflow transport during El Niño years. Previous studies have concluded that the ITF is affected by the latitudinal shifts of the North Equatorial Current (NEC) Bifurcation (Gordon et al., 2012; Kim et al., 2004), induced by the surface wind over the western tropical Pacific Ocean (Qiu & Lukas, 1996; Qu & Lukas, 2003; Qiu and Chen., 2010; Wei et al., 2016). The thermocline layer of the ITF at Makassar Strait is directly influenced by the Mindanao Current (MC) influx into Sulawesi Sea (Gordon et al., 2019; Jiang et al., 2019; Li et al., 2019). The regression between thermocline layer inflow transport and Sea Surface Height anomaly (SSHa) over a large domain covering the Pacific and Indian Oceans (Figure 4a) confirms that the ITF inflow is highly correlated (r more than 0.6) with the SSHa in the western Pacific Ocean, which is driven by ENSO. Under El Niño conditions, SSHa over western Pacific Ocean decreases significantly, and NEC bifurcation moves northward, which leads to a stronger MC (Kim et al., 2004; Qiu & Lukas, 1996). According to the nonlinear inertia of currents flowing across a gap (Sheremet, 2001; van Sebille et al., 2009), a stronger MC produces less leakage into Sulawesi Sea. In addition, the nonlinear collision of the Mindanao and Halmahera Eddies, which are influenced by the relative strength of the MC and the NGCC, is also important for the leakage of the ITF (Wang & Yuan, 2012, 2014).

The inflow in the sub-thermocline layer (300–760 m) has significant positive correlation ($r = 0.55$) with the Niño 3.4 with a lag time about 13 months (Figure 3a). Compared with the upper layer, the positive correlation and longer response time of the lower layer transport to the Niño 3.4 implies that different mechanisms control the different layers across the inflow section. The ITF originates from low-latitude boundary currents, and the sub-thermocline water is partly derived from the South Pacific (Gordon, 1986; Gordon & Fine, 1996; Valsala et al., 2011; Yang et al., 2018). ENSO is the main factor governing the low-latitude boundary currents of the North and South Pacific Oceans (Kessler & McCreary, 1993; Lee & Fukumori, 2003; Qiu & Chen, 2010). South Pacific subtropical gyre sea level decreases 6 months after the mature phase of El Niño, while the North Pacific subtropical gyre sea level decreases leading the mature phase by about 6 months (Figure S6). The equatorial South Pacific dominates part of the ITF sources waters during El Niño years and lags El Niño events about 6 months (Ueki et al., 2003; Valsala & Maksyutov, 2011). Therefore, the ITF inflow sub-thermocline layer variability is likely influenced by South Pacific variations and lags ENSO by about 13 months. A possible pathway for South Pacific water into the Sulawesi Sea might be the westward North Equatorial Subsurface Current (NESC) flowing underneath the North Equatorial Counter Current (NECC), which was first identified by Yuan et al. (2014). Instead of the linear dynamics of Sverdrup theory, nonlinear processes in the western boundary currents (Wang & Yuan, 2012, 2014) allow for South Pacific water to be mixed into the NESC. In addition, the propagation of baroclinic Rossby waves over the north Pacific Ocean at different time scales may also lead to the lagged response of the ITF sub-thermocline to ENSO. Detailed analysis of this is beyond the scope of this paper and will be explored in future work.

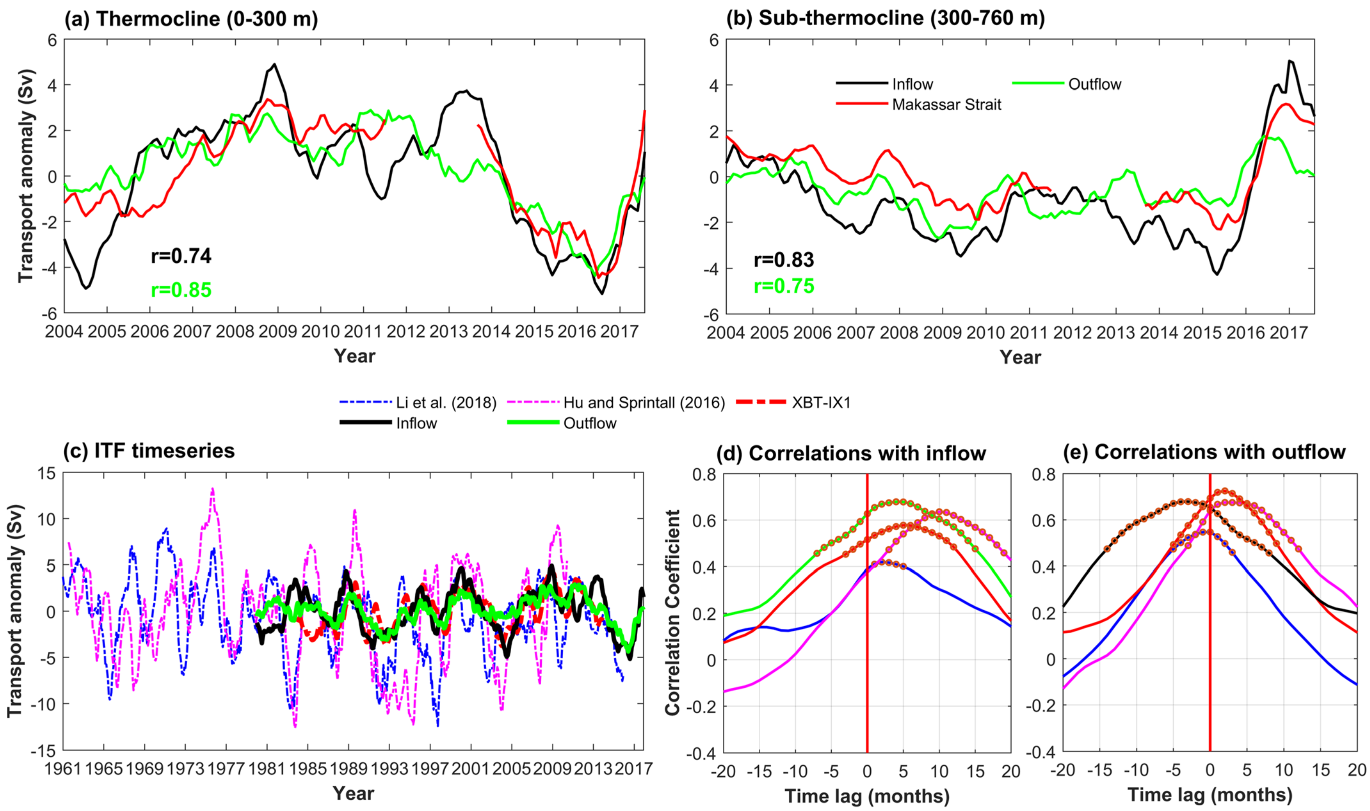

FIGURE 2. ITF timeseries validation. Comparison between ensemble inflow (black line)/outflow (green line) ITF timeseries and observed MST transport anomaly (red line) from 2004 to 2017 in the thermocline layer (a) and sub-thermocline layer (b). (c) Comparison between ensemble inflow (black line), outflow (green line) timeseries, and other ITF timeseries based on different schemes from previous studies. Firstly, XBT-IX1 outflow transport anomaly (red dashed line) based on XBT data at IX1 section (Liu et al., 2015). Secondly, Hu and Sprintall (2016) geostrophic transport anomaly calculated from EN4, ECMWF-ORA, and GFDL-ECDA (magenta line). Thirdly, Li et al. (2018) constructed 0–300 m Makassar Straits transport anomaly (blue dashed line) based on Pacific winds through neural network fitting. The positive values in figures (a–c) mean more southward (or westward) transport. All timeseries have been smoothed with a 13-month running mean. (d) Lead and lag correlations between three other ITF timeseries and inflow timeseries. (e) Same as (d) but for outflow timeseries. The orange dots represent the 95% confidence level determined using an effective degree of freedom.

From inflow timeseries (Figure 1c), the sub-thermocline layer inflow displays a sudden increase in transport anomaly after extreme El Niño events, such as 1982/1983, 1997/1998, and 2015/2016. Downwelling baroclinic Rossby waves generated and propagated into the western Pacific Ocean, along with an extreme El Niño event terminated in 2016, induced barotropic instability at the equatorial western Pacific Ocean and a weaker and more northward NECC (Qiu et al., 2019). This may lead to more South Pacific waters entering the eastern Sulawesi Sea. The regression between lower layer inflow transport and SSHa over a large domain covering the Pacific and Indian Oceans (Figure 4b) confirms that the inflow in the sub-thermocline layer is negatively correlated with the SSHa over the South Pacific subtropical gyre. Previous studies have indicated that the South Pacific subtropical gyre changes out of phase with North Pacific subtropical gyre in response to equatorial climate forcing (Wyrtki, 1974, 1989). Based on the different regression maps for the upper and lower layers, we propose that the ENSO-dependent variability of the northwestern Pacific Ocean plays a major role in the thermocline layer inflow, while the southwestern Pacific Ocean is the key region influencing the sub-thermocline layer inflow.

The thermocline transport of ITF outflow lags the Niño 3.4 about 5–7 months, which is consistent with conclusions based on IX1 data in Liu et al. (2015). The variations of the outflow in the thermocline layer are smaller than the inflow, with the outflow lagging the inflow by 4–5 months with a significant correlation coefficient of 0.7 (Figures 2d and 2e). Many studies have indicated that the IOD plays a role in modulating the ITF transport since ITF is controlled by the pressure difference between the Pacific and Indian Ocean (Liu et al., 2015; Pujiana et al., 2019; Yuan et al., 2011, 2013). Pujiana et al. (2019) confirmed that the

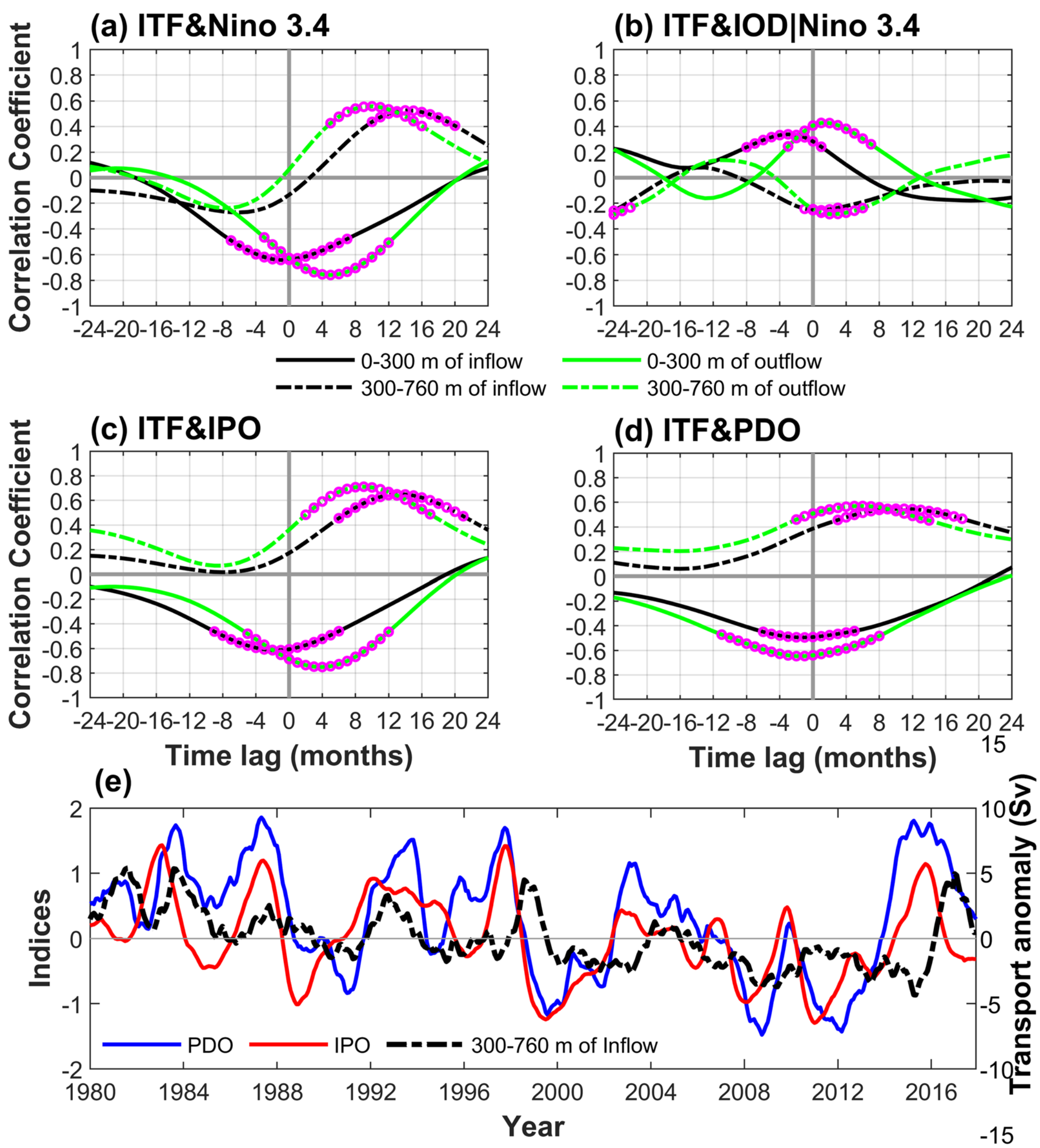

FIGURE 3. Lead and lag correlations between ITF inflow (outflow) variability and Indo-Pacific climate indices, (a) Niño 3.4; (b) partial correlations with IOD index (DMI) after remove the covariance with Niño 3.4 at 0 month; (c) IPO and (d) PDO index. The magenta dots represent 95% confidence level determined using an effective degree of freedom. (e) Comparison between the 13-month running mean sub-thermocline inflow variability (black line) and decadal climate modes (PDO-blue line and IPO-red line).

unprecedented decrease of ITF transport during 2016 was mainly due to a strong negative IOD event occurring in fall 2016. The correlations between ITF and IOD are significant when a partial correlation is preformed after removing the covariance with Niño 3.4 at 0 month (Figures 3b and S5). Thermocline layer ITF outflow positively responds to IOD with no lag and negatively responds to ENSO with 5–7 months lag, which implies that ENSO effect on the ITF can be weakened by Indian Ocean wind forcing related to the IOD (Feng et al., 2018; Gordon et al., 2019; Liu et al., 2015; Wijffels et al., 2008).

The outflow timeseries in the sub-thermocline layer exhibits an unexpected lag to ENSO, of about 7–9 months, a shorter lag time than the inflow (Figure 3a). This implies that the sub-thermocline ITF outflow changes may be significantly influenced by the eastern tropical Indian Ocean. From the regression map between sub-thermocline layer outflow transport and SSHa (Figure 4d), the eastern tropical Indian Ocean can negatively influence the ITF outflow in the sub-thermocline. The correlation coefficient between IOD

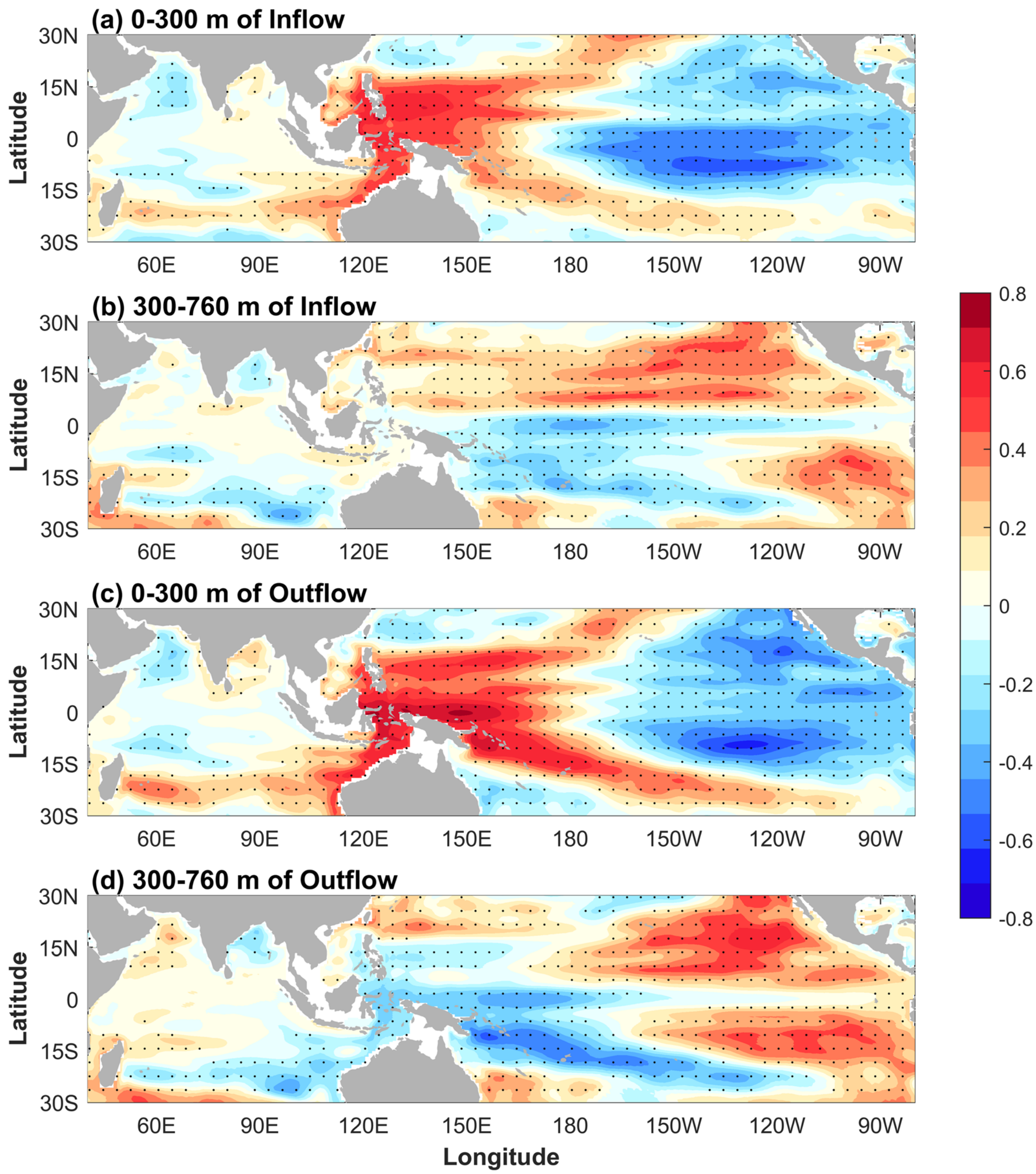

FIGURE 4. Regression maps of the ITF inflow and outflow variability to the SSHa. (a) Thermocline layer and (b)sub-thermocline layer of the inflow. (c) Thermocline layer and (d)sub-thermocline layer of the outflow. Stippling indicates significant correlation coefficients above the 95% confidence level.

and sub-thermocline ITF outflow is about −0.3 but also significant, with just 1–2 months lag (Figure 3b). There exist anomalous eastward currents in the sub-thermocline layer, which can transfer Indian Ocean signal and influence the ITF outflow (Figure S7). Previous studies have indicated that after the 1950s, there was a negative correlation between IOD and ENSO with the IOD leading more than 1 year (Clarke & Gorder, 2003; Izumo et al., 2010; Wang, 2019). This suggests that IOD events may cause ENSO events in the tropical Pacific with a time delay. A leading IOD signal combined with ITF outflow transports results to an earlier response to ENSO than inflow at sub-thermocline. The ITF also can feedback onto climate variability by modulating the temperature and salinity in the tropical Pacific and Indian Oceans (Kajtar et al., 2015). Positive correlation between IOD and ENSO is increased after the effect of ITF outflow is removed using partial correlation. After removing the influence of ITF inflow, IOD leads Niño 3.4 by about 3 months (Figure S8). This feature suggests that the ITF ocean pathway acts to weaken the relationship between IOD and ENSO.

On interannual to decadal time scales, the IPO and the PDO are the dominant climate forcing over Pacific Ocean. The correlation between the upper 300 m inflow and outflow transports and IPO index are similar to Niño 3.4. The lower layers of inflow and outflow are better correlated with the IPO (outflow: $r = 0.73$, lag of 7–9 months; inflow: $r = 0.67$, lag of 12–13 months) than with Niño 3.4 (Figure 3c). As for the PDO index, thermocline layer inflow and outflow negatively correlate ($r = -0.55$ for inflow and -0.63 for outflow) with PDO at zero lead/lag, while the sub-thermocline layer inflow is positively correlated with PDO ($r = 0.6$) with 5–10 months lag (Figure 3d). This indicates that the sub-thermocline transport variability is more sensitive to decadal climate forcing, especially the IPO. The 38-year inflow timeseries shows that the PDO, IPO, and sub-thermocline layer ITF have similar longer-term variability and trend (Figure 3e). The regression map of inflow/outflow time series with SSHa also shows that the tropical Southwest Pacific area is a key region for the sub-thermocline layer for both inflow and outflow (Figure 4).

4. Conclusions

Based on 2004–2017 Makassar Strait mooring data, 1980–2017 GODAS and SODA3 reanalysis, and OFES output, we analyze the interannual to decadal response of the ITF vertical profile to Indo-Pacific climate forcing through ensemble Pacific Ocean inflow and Indian Ocean outflow. The inflow and outflow timeseries are consistent with observed Makassar Strait data, XBT data at IX1 section, and other constructed timeseries from previous studies. The response time for the thermocline and sub-thermocline layers of inflow and outflow to Indo-Pacific climate forcing is different. The thermocline inflow responds negatively to Niño 3.4 with almost no lag, while the thermocline outflow lags by 5–7 months. The sub-thermocline inflow, which is influenced by both the North and South Pacific Oceans, positively responds to ENSO and IPO indices after 1 year and shows a significant long-term trend in agreement with IPO. Governed by both Pacific and Indian climate forcing, the sub-thermocline outflow positively correlates with the ENSO and IPO indices with about 7–9 months lag. ENSO effect on the ITF might be weakened by the Indian Ocean wind forcing related to the IOD as the ITF outflow negatively responds to ENSO, while positively responds to IOD.

Acknowledgments
We would like to thank Prof. M. Feng for sharing the XBT-IX1 ITF timeseries. We would also like to thank Dr. Shijian Hu for providing the geostrophic transport timeseries. This work was supported by the National Natural Science Foundation of China (Grants 41906004, 91958101, and 41976007) and the Fundamental Research Funds for the Central Universities (Grant 19lgpy32). The funding for ALG is derived from the NOAA Division of Ocean Observing and Monitoring, US Department of Commerce, award number UCAR Z15-17551. The statements, findings, conclusions, and recommendations are those of the authors and do not necessarily reflect the views of NOAA or the Department of Commerce. L.K.G. was supported by NASA Headquarters under the NASA Earth and Space Science Fellowship Program-Grant 80NSSC17K0438 Response of the Indian Ocean to Indonesian Throughflow Variability, the Lamont-Doherty Earth Observatory contribution number 8402. The Makassar Strait data are available online (https://www.ldeo.columbia.edu/~bhuber/MITF/). The GODAS data are obtained from Climate Prediction Center website (http://www.cpc.ncep.noaa.gov/products/GODAS), OFES data are available at the website (http://apdrc.soest.hawaii.edu/datadoc/ofes/ofes.php), and SODA 3.12.2 data can be downloaded at the website (http://dsrs.atmos.umd.edu/DATA/soda3.12.2/REGRIDED/ocean/). The Niño 3.4, IOD, PDO, and IPO indices are from the NOAA Earth System Research Laboratory (https://www.esrl.noaa.gov/psd/gcos_wgsp/Timeseries/).

References

Atmadipoera, A., Molcard, R., Madec, G., Wijffels, S., Sprintall, J., Koch-Larrouy, A., et al. (2009). Characteristics and variability of the Indonesian Throughflow water at the outflow straits. *Deep Sea Research*, *56*(11), 1942–1954. https://doi.org/10.1016/j.dsr.2009.06.004

Cai, W., van Rensch, P., Cowan, T., & Hendon, H. H. (2012). An asymmetry in the IOD and ENSO teleconnection pathway and its impact on Australian climate. *Journal of Climate*, *25*(18), 6318–6329. https://doi.org/10.1175/JCLI-D-11-00501.1

Clarke, A. J., & Gorder, S. V. (2003). Improving El Niño prediction using a space-time integration of indo-pacific winds and equatorial pacific upper ocean heat content. *Geophysical Research Letters*, *30*(30), 1399. https://doi.org/10.1029/2002GL016673.

Clarke, A. J., & Liu, X. (1994). Interannual sea level in the Northern and Eastern Indian Ocean. *Journal of Physical Oceanography*, *24*(6), 1224–1235. https://doi.org/10.1175/1520-0485(1994)024<1224:ISLITN>2.0.CO;2

Du, Y., & Qu, T. (2010). Three inflow pathways of the Indonesian throughflow as seen from the simple ocean data assimilation. *Dynamics of Atmospheres and Oceans*, *50*(2), 233–256. https://doi.org/10.1016/j.dynatmoce.2010.04.001

Duan, J., Li, Y., Wang, F., & Chen, Z. (2019). Decadal variations of the Mindanao current during 1960–2010. *Journal of Geophysical Research: Oceans*, *124*, 2660–2678. https://doi.org/10.1029/2019JC014975

England, M. H., Mcgregor, S., Spence, P., Meehl, G. A., Timmermann, A., Cai, W., et al. (2014). Recent intensification of wind-driven circulation in the Pacific and the ongoing warming hiatus. *Nature Climate Change*, *4*(3), 222–227. https://doi.org/10.1038/nclimate2106

Feng, M., Böning, C., Biastoch, A., Behrens, E., Weller, E., & Masumoto, Y. (2011). The reversal of the multi-decadal trends of the equatorial Pacific easterly winds, and the Indonesian throughflow and Leeuwin current transports. *Geophysical Research Letters*, *38*, 63. https://doi.org/10.1029/2011GL047291

Feng, M., Zhang, N., Liu, Q., & Wijffels, S. (2018). The Indonesian throughflow, its variability and centennial change. *Geoscience Letters*, *5*(1), 1–10. https://doi.org/10.1186/s40562-018-0102-2

Gordon, A., Susanto, R., & Vranes, K. (2003). Cool Indonesian Throughflow as a consequence of restricted surface layer flow. *Nature*, *425*(2003), 824–828. https://doi.org/10.1038/nature02038

Gordon, A., Sprintall, J., Van Aken, H., Susanto, D., Wijffels, S., Molcard, R., et al. (2010). The Indonesian throughflow during 2004–2006 as observed by the INSTANT program. *Dynamics of Atmospheres and Oceans*, *50*(2), 115–128. https://doi.org/10.1016/j.dynatmoce.2009.12.002

Gordon, A. L. (1986). Interocean exchange of thermocline water. *Journal of Geophysical Research*, *91*(C4), 5037–5046. https://doi.org/10.1029/JC091iC04p05037

Gordon, A. L. (2001). Chapter 4.7 Interocean exchange. *International Geophysics*, *77*(01), 303–314. https://doi.org/10.1016/S0074-6142(01)80125-X

Gordon, A. L., & Fine, R. A. (1996). Pathways of water between the Pacific and Indian oceans in the Indonesian seas. *Nature*, *379*(6561), 146–149. https://doi.org/10.1038/379146a0

Gordon, A. L., Huber, B. A., Metzger, E. J., Susanto, R. D., Hurlburt, H. E., & Adi, T. R. (2012). South China Sea throughflow impact on the Indonesian throughflow. *Geophysical Research Letters*, *39*, 90. https://doi.org/10.1029/2012GL052021

Gordon, A. L., Napitu, A., Huber, B. A., Gruenburg, L. K., Pujiana, K., Agustiadi, T., et al. (2019). MST seasonal and interannual variability, an overview. *Journal of Geophysical Research: Oceans*, *124*, 3724–3736. https://doi.org/10.1029/2018JC014502

Gordon, A. L., Susanto, R., Ffield, A., Huber, B., Pranowo, W., & Wirasantosa, S. (2008). Makassar Strait Throughflow, 2004 to 2006. *Geophysical Research Letters*, *35*, L24605. https://doi.org/10.1029/2008GL036372

Gordon, A. L., Susanto, R. D., & Ffield, A. (1999). Throughflow within Makassar Strait. *Geophysical Research Letters*, *26*(21), 3325–3328. https://doi.org/10.1029/1999GL002340

Gruenburg, L. K., & Gordon, A. L. (2018). Variability in Makassar Strait heat flux and its effect on the eastern tropical Indian Ocean. *Oceanography*, *31*(2), 80–87. https://doi.org/10.5670/oceanog.2018.220

Hu, D., Wu, L., Cai, W., Gupta, A. S., Ganachaud, A., Qiu, B., et al. (2015). Pacific western boundary currents and their roles in climate. *Nature*, *522*(7556), 299–308. https://doi.org/10.1038/nature14504

Hu, S., & Sprintall, J. (2016). Interannual variability of the Indonesian Throughflow: The salinity effect. *Journal of Geophysical Research: Oceans*, *121*, 2596–2615. https://doi.org/10.1002/2015JC011495

Hu, S., & Sprintall, J. (2017). Observed strengthening of interbasin exchange via the Indonesian seas due to rainfall intensification. *Geophysical Research Letters*, *44*, 1448–1456. https://doi.org/10.1002/2016GL072494

Izumo, T., Vialard, J., Lengaigne, M., Montegut, C., & Yamagata, T. (2010). Influence of the state of the Indian Ocean dipole on the following years El Niño. *Nature Geoscience*, *3*(3), 168–172. https://doi.org/10.1038/ngeo760

Jiang, G. Q., Wei, J., Malanotte-Rizzoli, P., Li, M., & Gordon, A. L. (2019). Seasonal and interannual variability of the subsurface velocity profile of the Indonesian Throughflow at Makassar Strait. *Journal of Geophysical Research: Oceans*, *124*, 9644–9657. https://doi.org/10.1029/2018JC014884

Kajtar, J. B., Santoso, A., England, M. H., & Cai, W. (2015). Indo-pacific climate interactions in the absence of an Indonesian throughflow. *Journal of Climate*, *28*(13), 5017–5029. https://doi.org/10.1175/JCLI-D-14-00114.1

Kessler, W., & McCreary, J. (1993). The annual wind-driven Rossby wave in the subthermocline equatorial Pacific. *Journal of Physical Oceanography*, *23*(6), 1192–1207. https://doi.org/10.1175/1520-0485(1993)023<1192:TAWDRW>2.0.CO;2

Kim, Y. Y., Qu, T., Jensen, T., Miyama, T., Mitsudera, H., Kang, H.-W., & Ishida, A. (2004). Seasonal and interannual variations of the north equatorial current bifurcation in a high-resolution OGCM. *Journal of Geophysical Research*, *109*, C03040. https://doi.org/10.1029/2003JC002013

Lee, S.-K., Park, W., Baringer, M. O., Gordon, A. L., Huber, B., & Liu, Y. (2015). Pacific origin of the abrupt increase in Indian Ocean heat content during the warming hiatus. *Nature Geoscience*, *8*(6), 445–449. https://doi.org/10.1038/ngeo2438

Lee, T., & Fukumori, I. (2003). Interannual to decadal variation of tropical-subtropical exchange in the Pacific Ocean: Boundary versus interior pycnocline transports. *Journal of Climate*, *16*(24), 4022–4042. https://doi.org/10.1175/1520-0442(2003)016<4022:IVOTEI>2.0.CO;2

Li, M., Gordon, A. L., Wei, J., Gruenburg, L. K., & Jiang, G. (2018). Multi-decadal timeseries of the Indonesian Throughflow. *Dynamics of Atmospheres and Oceans*, *81*, 84–95. https://doi.org/10.1016/j.dynatmoce.2018.02.001

Li, M., Wei, J., Wang, D., Gordon, A. L., Yang, S., Malanotte-Rizzoli, P., & Jiang, G. (2019). Exploring the importance of the Mindoro-Sibutu pathway to the upper-layer circulation of the South China Sea and the Indonesian Throughflow. *Journal of Geophysical Research: Oceans*, *124*, 5054–5066. https://doi.org/10.1029/2018JC014910

Liu, Q. Y., Feng, M., Wang, D., & Wijffels, S. (2015). Interannual variability of the Indonesian throughflow transport: A revisit based on 30-year expendable bathythermograph data. *Journal of Geophysical Research: Oceans*, *120*, 8270–8282. https://doi.org/10.1002/2015JC011351

Masumoto, Y. (2002). Effects of interannual variability in the eastern Indian Ocean on the Indonesian Throughflow. *Journal of Oceanography*, *58*(1), 175–182. https://doi.org/10.1023/A:1015889004089

Masumoto, Y., Sasaki, H., Kagimoto, T., Komori, N., Ishida, A., Sasai, Y., et al. (2004). A fifty-year eddy-resolving simulation of the world ocean: Preliminary outcomes of OFES (OGCM for the earth simulator). *Journal of the Earth Simulator*, *1*(April), 35–56.

Murtugudde, R., Busalacchi, A. J., & Beauchamp, J. (1998). Seasonal-to-interannual effects of the indonesian throughflow on the tropical indo-pacific basin. *Journal of Geophysical Research*, *103*(C10), 21,425–21,441. https://doi.org/10.1029/98JC02063

Nieves, V., Willis, J. K., & Patzert, W. C. (2015). Recent hiatus caused by decadal shift in indo-pacific heating. *Science*, *349*(6247), 532–535. https://doi.org/10.1126/science.aaa4521

Potemra, J. T., & Schneider, N. (2007). Influence of low-frequency indonesian throughflow transport on temperatures in the indian ocean in a coupled model*. *Journal of Climate*, *20*(7), 1339–1352. https://doi.org/10.1175/JCLI4146.1

Pujiana, K., Gordon, A. L., & Sprintall, J. (2013). Intraseasonal kelvin wave in Makassar Strait. *Journal of Geophysical Research: Oceans*, *118*, 2023–2034. https://doi.org/10.1002/jgrc.20069

Pujiana, K., McPhaden, M. J., Gordon, A. L., & Napitu, A. M. (2019). Unprecedented response of Indonesian throughflow to anomalous Indo-Pacific climatic forcing in 2016. *Journal of Geophysical Research: Oceans*, *124*, 3737–3754. https://doi.org/10.1029/2018JC014574

Qiu, B., & Chen, S. (2010). Interannual-to-decadal variability in the bifurcation of the north equatorial current off the Philippines. *Journal of Physical Oceanography*, *40*(11), 2525–2538. https://doi.org/10.1175/2010JPO4462.1

Qiu, B., Chen, S., Powell, B., Colin, P. L., Rudnick, D. L., & Schonau, M. C. (2019). Nonlinear short-term upper ocean circulation variability in the tropical western Pacific. *Oceanography*, *32*(4), 22–31. https://doi.org/10.5670/oceanog.2019.408

Qiu, B., & Lukas, R. (1996). Seasonal and interannual variability of the north equatorial current, the Mindanao current, and the Kuroshio along the Pacific western boundary. *Journal of Geophysical Research: Oceans*, *101*(C5), 12,315–12,330. https://doi.org/10.1029/95JC03204

Qu, T., & Lukas, R. (2003). The bifurcation of the north equatorial current in the Pacific. *Journal of Physical Oceanography*, *33*(1), 5–18. https://doi.org/10.1175/1520-0485(2003)033<0005:TBOTNE>2.0.CO;2

Ren, Q., Li, Y., Wang, F., Song, L., Liu, C., & Zhai, F. (2018). Seasonality of the Mindanao current/undercurrent system. *Journal of Geophysical Research: Oceans*, *123*, 1105–1122. https://doi.org/10.1002/2017JC013474

Santoso, A., England, W. C., & Phipps, S. J. (2011). The role of the Indonesian throughflow on ENSO dynamics in a coupled climate model. *Journal of Climate*, *24*(3), 585–601. https://doi.org/10.1175/2010JCLI3745.1

Sprintall, J., Gordon, A. L., Murtugudde, R., & Susanto, R. D. (2000). A semiannual Indian Ocean forced kelvin wave observed in the Indonesian seas in May 1997. *Journal of Geophysical Research*, *105*, 17,217–17,230. https://doi.org/10.1029/2000JC900065

Sheremet, V. A. (2001). Hysteresis of a Western boundary current leaping across a gap. *Journal of Physical Oceanography*, *31*(5), 1247–1259. https://doi.org/10.1175/1520-0485(2001)031<1247:HOAWBC>2.0.CO;2

Song, Q., & Gordon, A. (2004). Significance of the vertical profile of Indonesian Throughflow transport on the Indian Ocean. *Geophysical Research Letters*, *31*, L16307. https://doi.org/10.1029/2004GL020360

Sprintall, J., Gordon, A. L., Koch-Larrouy, A., Lee, T., Potemra, J. T., Pujiana, K., & Wijffels, S. E. (2014). The Indonesian seas and their role in the coupled ocean–climate system. *Nature Geoscience*, *7*(7), 487–492. https://doi.org/10.1038/ngeo2188
Sprintall, J., & Révelard, A. (2014). The Indonesian Throughflow response to Indo-Pacific climate variability. *Journal of Geophysical Research: Oceans*, *119*, 1161–1175. https://doi.org/10.1002/2013JC009533
Sprintall, J., Wijffels, S. E., Molcard, R., & Jaya, I. (2009). Direct estimates of the indonesian throughflow entering the indian ocean: 2004–2006. *Journal of Geophysical Research*, *114*, C07001. https://doi.org/10.1029/2008JC005257
Stuecker, M. F., Timmermann, A., Jin, F.-F., Chikamoto, Y., Zhang, W., Wittenberg, A. T., et al. (2017). Revisiting ENSO/Indian OceanDipole phase relationships. *Geophysical Research Letters*, *44*, 2481–2492. https://doi.org/10.1002/2016GL072308
Susanto, R. D., Ffield, A., Gordon, A. L., & Adi, T. R. (2012). Variability of Indonesian throughflow within Makassar Strait, 2004–2009. *Journal of Geophysical Research*, *117*, 47. https://doi.org/10.1029/2012JC008096
Tillinger, D., & Gordon, A. L. (2010). Fifty years of the Indonesian throughflow*. *Journal of Climate*, *22*(23), 6342–6355.
Ueki, I., Kashino, Y., & Kuroda, Y. (2003). Observation of current variations off the New Guinea coast including the 1997-1998 El Niño period and their relationship with Sverdrup transport. *Journal of Geophysical Research*, *108*(C7), 61. https://doi.org/10.1029/2002jc001611
Valsala, V., Maksyutov, S., & Murtugudde, R. (2011). Interannual to interdecadal variabilities of the Indonesian Throughflow source water pathways in the Pacific Ocean. *Journal of Physical Oceanography*, *41*(10), 1921–1940. https://doi.org/10.1175/2011JPO4561.1
van Sebille, E., Biastoch, A., van Leeuwen, P. J., & de Ruijter, W. P. M. (2009). A weaker Agulhas current leads to more Agulhas leakage. *Geophysical Research Letters*, *36*, L03601. https://doi.org/10.1029/2008GL036614
Wang, C. (2019). Three-ocean interactions and climate variability: A review and perspective. *Climate Dynamics*, *53*(7–8), 5119–5136. https://doi.org/10.1007/s00382-019-04930-x
Wang, L. C., & Wu, C. R. (2013). Contrasting the flow patterns in the equatorial pacific between two types of El Niño. *Atmosphere-Ocean*, *51*(1), 60–74. https://doi.org/10.1080/07055900.2012.744294
Wang, Z., & Yuan, D. (2012). Nonlinear dynamics of two western boundary currents colliding at a gap. *Journal of Physical Oceanography*, *42*(11), 2030–2040. https://doi.org/10.1175/JPO-D-12-05.1
Wang, Z., & Yuan, D. (2014). Multiple Equilibria and hysteresis of two unequal-transport western boundary currents colliding at a gap. *Journal of Physical Oceanography*, *44*(7), 1873–1885. https://doi.org/10.1175/JPO-D-13-0234.1
Wei, J., Li, M. T., Malanotte-Rizzoli, P., Gordon, A. L., & Wang, D. X. (2016). Opposite variability of Indonesian Throughflow and South China Sea Throughflow in the Sulawesi Sea. *Journal of Physical Oceanography*, *46*(10), 3165–3180. https://doi.org/10.1175/JPO-D-16-0132.1
Wijffels, S., Meyers, G., & Godfrey, J. S. (2008). A twenty year average of the Indonesian Throughflow: Regional currents and the interbasin exchange. *Journal of Physical Oceanography*, *38*(9), 1965–1978. https://doi.org/10.1175/2008JPO3987.1
Wyrtki, K. (1965). Surface currents of the eastern tropical Pacific Ocean. *Inter-American Tropical Tuna Commission Bulletin*, *9*(1965), 271–304.
Wyrtki, K. (1974). Equatorial currents in the pacific 1950 to 1970 and their relations to the trade winds. *Journal of Physical Oceanography*, *4*(3), 372–380. https://doi.org/10.1175/1520-0485(1974)004<0372:ECITPT>2.0.CO;2
Wyrtki, K. (1987). Indonesian Throughflow and the associated pressure gradient. *Journal of Geophysical Research*, *92*(C12), 12,941–12,946. https://doi.org/10.1029/JC092iC12p12941
Wyrtki, K. (1989). Some thoughts about the West Pacific Warm Pool. In: J. Picaut, et al. (Eds.), Proc. of Western Pacific International Meeting and Workshop on TOGA COARE. Centre de Noumea, New Caledonia, pages 99-109.
Yang, L., Zhou, L., Li, S., & Wei, Z. (2018). Spreading of the South Pacific tropical water and Antarctic intermediate water over the maritime continent. *Journal of Geophysical Research: Oceans*, *123*, 4423–4446. https://doi.org/10.1029/2018JC013831
Yuan, D., Li, X., Wang, Z., Li, Y., Wang, J., Yang, Y., et al. (2018). Observed transport variations in the Maluku Channel of the Indonesian seas associated with western boundary current changes. *Journal of Physical Oceanography*, *48*(8), 1803–1813. https://doi.org/10.1175/JPO-D-17-0120.1
Yuan, D., Wang, J., Xu, T., Xu, P., Hui, Z., Zhao, X., et al. (2011). Forcing of the Indian Ocean dipole on the interannual variations of the tropical Pacific Ocean: Roles of the Indonesian Throughflow. *Journal of Climate*, *24*(14), 3593–3608. https://doi.org/10.1175/2011JCLI3649.1
Yuan, D., Zhang, Z., Chu, P. C., & Dewar, W. K. (2014). Geostrophic circulation in the tropical North Pacific Ocean based on Argo profiles. *Journal of Physical Oceanography*, *44*(2), 558–575. https://doi.org/10.1175/JPO-D-12-0230.1
Yuan, D., Zhou, H., & Zhao, X. (2013). Interannual climate variability over the tropical Pacific Ocean induced by the Indian Ocean dipole through the Indonesian Throughflow. *Journal of Climate*, *26*(9), 2845–2861. https://doi.org/10.1175/JCLI-D-12-00117.1